

## CHAPTER 21

### TRUNCATION ORDER OF FOURIER WAVE THEORY

Rodney J. Sobey<sup>1</sup>, M.ASCE

Specific consideration is given to the dependence of Fourier wave solutions on both truncation order and the number of free surface nodes. Solution dependence is quantified by a comprehensive set of numerical experiments over a typical range of wave height, water depth, truncation order and overspecification values. Integral error measures include the rms free surface boundary condition errors and a slope error that identifies non-physical positive slope segments in the wave profile between crest and trough. Summary error diagrams are presented as a guide to the adoption of suitable truncation orders and overspecification for Fourier solutions. The truncation order is the crucial parameter but there is measurable advantage in some small overspecification.

#### INTRODUCTION

Fourier wave theory has proved to be a robust steady wave theory for almost the complete range of wave heights, water depths and uniform currents experienced in practice. It is a hybrid analytical/numerical theory. The analytical aspects are relatively straightforward though not entirely without difficulties. The numerical part of the solution however is distinctly nontrivial. It involves the simultaneous solution of a large number of implicit nonlinear algebraic equations in a large number of unknowns. This is recognized as an extremely difficult problem in numerical analysis for which a successful solution algorithm depends critically on the analytical formulation of the problem and on the physical nature of the solution. For waves of small to moderate height in relatively deep water, successful solutions do not appear to be difficult to obtain. For higher waves in deep water and especially waves of moderate to large height in shallow water, changes in the physical nature of the solution significantly complicate the achievement of a successful solution. So much so in fact that it becomes appropriate to consider just what is a successful solution. The complexity of the numerical solution procedure has tended to distract attention from this rather more fundamental question, namely, whether an achievable numerical solution can be equated with a reasonable physical solution of a particular steady wave problem.

#### STEADY WAVE THEORY

Progressive waves of permanent form are steady in a frame of reference moving at the phase speed  $C$ . Accordingly, it is convenient to adopt a steady and moving  $x,z$  reference frame that is located at the mean water level (MWL) and moves at speed  $C$  with the wave crest, rather than an unsteady and fixed  $X,Z$  reference frame. The field solution is described by the stream function  $\psi(x,z)$ . Assuming that the flow is incompressible and irrotational, the field equation representing mass and momentum conservation is the Laplace equation

---

<sup>1</sup> Professor, Hydraulic and Coastal Group, Department of Civil Engineering, University of California at Berkeley, Berkeley, CA 94720

$$\frac{\partial^2 \Psi}{\partial x^2} + \frac{\partial^2 \Psi}{\partial z^2} = 0 \quad (1)$$

where the velocity components ( $u, w$ ) are  $(\partial \Psi / \partial z, -\partial \Psi / \partial x)$ .

This field equation is subject to the following boundary conditions:

(1) Bottom boundary condition, representing no flow through the horizontal bed, is

$$\Psi(x, -h) = 0 \quad \text{at } z = -h \quad (2)$$

(2) Kinematic free-surface boundary condition (KFSBC), representing no flow through the free surface, is

$$\Psi(x, \eta) = -Q \quad \text{at } z = \eta(x) \quad (3)$$

where  $\eta(x)$  is the free surface and  $-Q$  is the constant volume flow rate per unit width under the steady wave.  $Q$  is positive and this flow is in the negative  $x$  direction.

(3) Dynamic free surface boundary condition (DFSBC), representing constant atmospheric pressure on the free surface, is

$$\frac{1}{2} \left( \frac{\partial \Psi}{\partial x} \right)^2 + \frac{1}{2} \left( \frac{\partial \Psi}{\partial z} \right)^2 + g \eta = R \quad \text{at } z = \eta(x) \quad (4)$$

where  $g$  is the gravitational acceleration and  $R$  the Bernoulli constant.

(4) Wave is periodic.

$$\Psi(x + L, z) = \Psi(x, z) \quad (5)$$

where  $L (= 2\pi/k)$  is the wave length and  $k$  is the wave number

Given parameters defining a steady wave solution are generally the wave height  $H$ , the water depth  $h$ , the wave period  $T (= 2\pi/\omega)$  and either the coflowing Eulerian current  $C_E$  or the wave-averaged mass transport velocity or Stokes drift  $C_S$ . The wave height is defined as

$$H = \eta(x=0) - \eta(x=L/2) \quad (6)$$

and mass conservation requires an invariant MWL such that

$$\int_0^{L/2} \eta(x) dx = 0 \quad (7)$$

The speed  $C$  of the moving and steady reference frame is related to the fixed and unsteady reference frame by the dispersion relationship. Where  $C_E$  is known, the dispersion relationship is

$$C = \frac{L}{T} = \bar{u} + C_E \quad (8)$$

where  $\bar{u}$  is the mean fluid speed at any  $z$  wholly within the fluid. The Stokes drift is then defined as

$$C = \frac{L}{T} = \frac{Q}{h} + C_S \quad (9)$$

Where  $C_S$  is known, Equation 9 is the dispersion relationship and Equation 8 is the definition equation for  $C_E$ .

## FOURIER WAVE THEORY

The solution for the stream function is represented by a truncated Fourier series

$$\Psi(x, z) = -\bar{u}z + \frac{g^2}{\omega^3} \sum_{j=1}^N B_j \frac{\sinh jk(h+z)}{\cosh jkh} \cos jkx \quad (10)$$

where the  $B_j$  are the dimensionless Fourier coefficients, of which there are  $N$ . This representation of the stream function automatically satisfies the field equation, the kinematic bottom boundary condition and the periodic lateral boundary conditions. The Fourier coefficients are chosen numerically to satisfy the free surface boundary conditions, the finite truncation order  $N$  being the only necessary assumption in the analytical formulation of Fourier wave theory.

The unknown variables in a Fourier wave solution are  $k, \bar{u}, C_E$  or  $C_S, Q, R$ , the  $\eta_m$  for  $m=0(1)M$  and  $B_j$  for  $j=1(1)N$ , of which there are  $M+N+6$  in total. The  $\eta_m = \eta(x_m)$  are water surface nodes, where the  $x_m = (m-1)\pi/kM$  are uniformly distributed in  $x$  from crest to trough.

The problem formulation provides  $2M+6$  implicit algebraic equations in these  $M+N+6$  unknowns, each equation being cast in the form

$$f_i(k, \bar{u}, C_E \text{ or } C_S, Q, R, \eta_m, B_j) = 0 \quad (11)$$

The equations define the wave height

$$f_1 = \eta_0 - \eta_M - H \quad (12)$$

the mean water level

$$f_2 = \frac{1}{2M} \left( \eta_0 + 2 \sum_{m=1}^{M-1} \eta_m + \eta_M \right) \quad (13)$$

the Eulerian current

$$f_3 = \frac{2\pi/k}{T} - \bar{u} - C_E \quad (14)$$

the Stokes drift

$$f_4 = \frac{2\pi/k}{T} - \frac{Q}{h} - C_S \quad (15)$$

the kinematic free surface boundary condition (KFSBC) at each of the  $M+1$  free surface nodes

$$f_{5+2m} = \Psi(x_m, \eta_m) + Q \quad (16)$$

and the dynamic free surface boundary condition (DFSBC) also at each of the free surface nodes

$$f_{6+2m} = \frac{1}{2} \left[ \frac{\partial \Psi(x_m, \eta_m)}{\partial x} \right]^2 + \frac{1}{2} \left[ \frac{\partial \Psi(x_m, \eta_m)}{\partial z} \right]^2 + g \eta_m - R \quad (17)$$

Note in particular the use of the trapezoidal rule in Equation 13 for the MWL. This is an exact result for the continuous integral in Equation 7 where  $\eta(x)$  is represented by a truncated Fourier series, as is implied by Equation 10.

The problem is uniquely defined for  $M = N$  and overspecified for  $M > N$ . The solution of a set of  $2N+6$  simultaneous implicit algebraic equations in  $2N+6$  unknowns is a familiar problem in numerical analysis for which successful algorithms are generally variations on the Newton-Raphson method. A set of  $2N+6$  simultaneous implicit algebraic equations in  $M+N+6$  unknowns, where  $M > N$ , is an equally familiar problem in numerical analysis in the context of nonlinear optimization. A solution is established by seeking a minimum value for an objective function of the  $M+N+6$  unknowns. A familiar algorithm is the least squares method where the objective function is the sum of squares of the left hand sides of the  $2M+6$  equations.

$$O(k, \bar{u}, C_E \text{ or } C_S, Q, R, \eta_m, B_j) = f_1^2 + f_2^2 + \dots + f_{2M+6}^2 \quad (18)$$

Such an algorithm is equally successful for  $M = N$  where the objective function would be expected to be zero. In practice, this involves little sacrifice in computational efficiency and none in solution precision and is accordingly a convenient choice of algorithm for the present purposes.

The choice of numerical solution algorithm should not influence the solution and the present computations have exclusively adopted the IMSL subroutine ZXSSQ, which is a finite-difference Levenberg-Marquardt algorithm with strict descent in double precision. This algorithm is mature, routinely successful and commonly available. Given that a solution exists, there are two potential difficulties with any optimization algorithm. The first is the difference in physical dimensions and relative magnitudes of the dependent variables. This has been minimized by redefining the variables and the implicit algebraic equations in dimensionless form, here in terms of  $\omega$  and  $g$ . Subse-

quently, all constants and variables are non-dimensional, simply achieved by setting  $\omega = g = \rho = 1$ . A second difficulty is the potential existence of multiple solutions, especially the odd harmonics which are legitimate mathematical solutions of the gravity wave problem as formulated. This problem can be avoided, for example, by the choice of an initial estimate of the complete solution from Airy wave theory at a fraction of the given wave height. The wave height is then progressively increased towards the given wave height, with an initial estimate at each subsequent step being provided by a Taylor series expansion in  $H$  about the converged solution at the previous height step. A fraction sequence of 0.01, 0.02, 0.05, 0.1, 0.2, 0.5, 1.0 has been employed, with two steps normally sufficient in very deep water, four in transitional water and all seven in extremely shallow water.

Whether a solution exists at all is a further potential difficulty and there are two aspects here that require attention. The first is the truncation order  $N$  of the Fourier series. Steep crest and flat trough profiles typical of shallow water waves require many more Fourier terms than the more closely sinusoidal wave profiles in deep water. The theoretical slope discontinuity at the crest of limit waves would require an infinite truncation order and can not be accommodated by Fourier wave theory; in practice however, adequate solutions can be achieved very close to this limit. The second aspect is whether or not a solution does indeed exist and here the problem formulation is remarkably prophetic and robust. Convergence is just not achieved for the present formulation, despite the mathematical possibility of a minimum of the objective function, at combinations of dependent variables that are not physically possible. This is an especially encouraging aspect of the problem formulation and the numerical solution, considering the extreme multi-dimensionality of the problem and the considerable potential for spurious solutions.

Previous formulations of Fourier wave theory (Dean 1965 & 1974, Dalrymple 1974, Chaplin 1980, Rienecker & Fenton 1981) have been reviewed in detail elsewhere (Sobey 1988) and compared with the present generalized formulation. Differences are more apparent than real. The Dean, Dalrymple and Chaplin algorithms lack some flexibility in excluding Stokes second definition of phase speed. The present algorithm is a modification (normalized by known wave frequency rather than unknown wave number) and generalization ( $M$  can be greater than  $N$ ) of the Fenton (1983) version of the Rienecker and Fenton formulation. All algorithms were shown to provide essentially identical results with Stokes first definition of phase speed for wave height up to at least 90% of the breaking wave height. The slope discontinuity for limit waves requires an infinite Fourier series which is beyond the capabilities of a truncated Fourier series. Substantially increasing the truncation order (Chaplin uses  $N=51$  at 90% of breaking wave height) improves fidelity for near-limit waves but finite machine precision rapidly limits the utility of this approach. Numerical solutions for nominally limit waves at finite truncation orders by Dean (1974) have been shown to be spurious solutions by Chaplin (1980), as they do not capture the dual-valued nature of integral properties of near-limit waves.

Given the essentially complete agreement among Fourier wave theory formulations for small to moderately extreme wave heights, the present generalized formulation can be utilized in an analysis of solution characteristics in the reasonable expectation that the results will be applicable also to alternative formulations. Limit waves can not be accommodated by any Fourier formulation and will not be included in the analysis, which will focus on small (Dean case A at 25% of empirical breaking wave height) and moderately extreme (Dean case C at 75% of empirical breaking wave height) waves.

## ERROR MEASURES

Fourier wave theory has but two assumptions, the truncation order  $N$  and the number of water surface steps  $M+1$ . Given that  $M$  must be greater than or equal to  $N$  for closure, it is convenient to define the overspecification  $MN = M - N$ . Both  $N$  and  $MN$  influence the fidelity of the solution and, being the only assumptions of the theory, there is considerable value in documenting the numerical solution dependence on both parameters. The influence of truncation order is implicit in most published solutions,

with adopted  $N$  values increasing from small to high waves and especially from deep to shallow water. The influence of  $MN$  is rather less obvious. Dean and Dalrymple do not record  $M$ , beyond a statement to the effect that  $M$  is large. Chaplin apparently uses  $M=200$  but Rienecker and Fenton use  $M=N$ , i.e.  $MN=0$ . In principle and frequently in practice, numerical solutions are achievable for all  $N \geq 1$  and all  $MN > 0$ . Spurious solutions may result from inappropriate choices of both  $N$  and  $MN$ . The truncation order is broadly analogous to order of an analytical waves theory such as Stokes or cnoidal; it should not be too small but what is large enough? Similarly, what is an appropriate value for  $MN$ ? It is implicit in the Dean, Dalrymple and Chaplin formulations that a "large" value of  $MN$  is essential for solution fidelity. How large is "large"? Some guidance in answering these questions can be provided from the analysis of numerical solutions over a range of  $N$  and  $MN$  values.

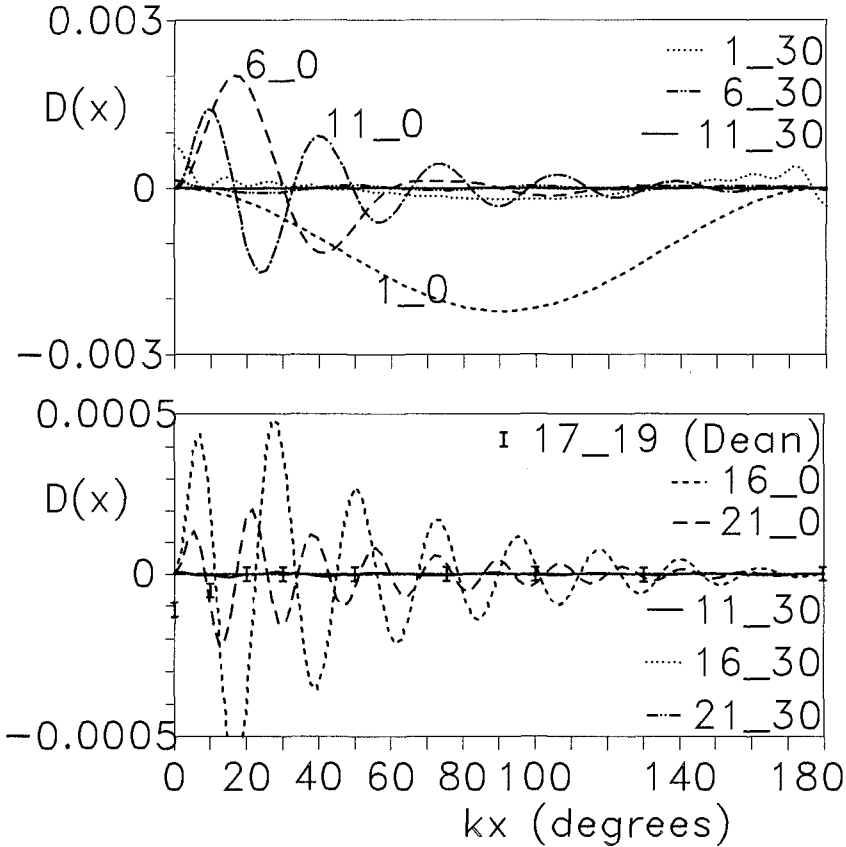


**Figure 1 DFSBC Error Traces for Case 3C**

Error measures must be defined to assist in this analysis. Two appropriate objective criteria follow naturally from the problem formulation, where only the free surface boundary conditions are not satisfied exactly. The residual error in the KFSBC is

$$K(x) = \psi(x, n) + Q \tag{19}$$

Similarly, the residual error in the DFSBC is

$$D(x) = \frac{1}{2} \left( \frac{\partial \psi}{\partial x} \right)^2 + \frac{1}{2} \left( \frac{\partial \psi}{\partial z} \right)^2 + g\eta - R \tag{20}$$

These error traces oscillate about zero in a manner typical of truncated Fourier series. The Fourier solution satisfies these boundary conditions at discrete, uniformly spaced surface nodes, not along the entire free surface. This is illustrated in Figure 1 for Dean Case 3C ( $\omega^2 h/g = 2\pi/100$ ;  $\omega^2 H/g = 0.03657$ ,  $C_n = 0$ ) for  $D(x)$  over a range of  $N$  and  $MN$ , each profile being based on 100 points between crest and trough. The truncation order influences these traces directly, there being exactly  $N$  oscillatory cycles per wavelength. For  $MN = 0$ , the zero crossings of the error traces identify the locations of the free surface nodes. Overspecification  $MN$  influences the phasing and amplitude of these traces, generally decreasing the amplitude of the oscillation, except where the truncation order is ridiculously small ( $N = 1$ ). The principal advantage of overspecification would appear to be the change in the phasing of the error traces; the free surface nodes are moved from the natural zero-crossings of the  $N$ -term finite Fourier series and the amplitude of the trace oscillations is damped significantly in consequence. The markers on Figure 1 are the published Dean (1974) solution (where  $N=17$ ,  $MN=36n-17$ ,  $n$  being an unrecorded integer). These errors are given to only one significant figure and are indicated by error bands, but are nonetheless entirely consistent with the present results. The phase reversal is apparently a consequence of the different numerical optimization algorithms and is not believed to be significant. In all cases except the trivial  $N = 1$ , the trace amplitude is a maximum at the crest and decays rapidly in magnitude towards the trough.

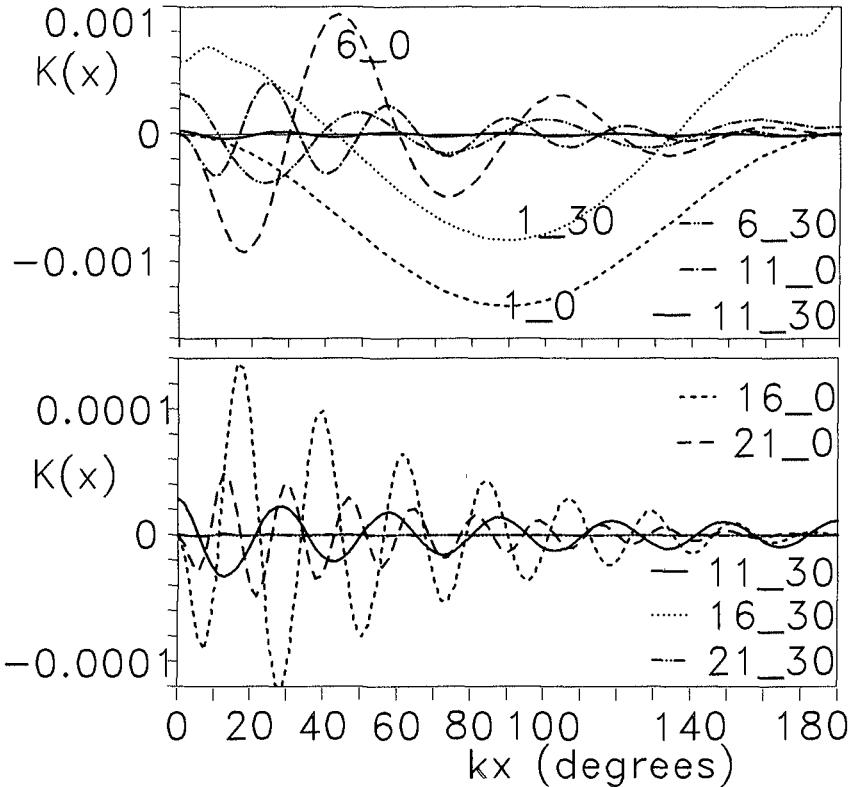


Figure 2 KFSBC Error Traces for Case 3C

The KFSBC error trace  $K(x)$  behaves similarly and is shown in Figure 2 for the same Dean case 3C solutions as in Figure 1. Dean (1965, 1974) defines the KFSBC errors as  $dn/dx - u/w$ , which is not directly comparable with Equation 19. It is emphasized in the Dean (1965, 1974) formulation of Fourier wave theory that the KFSBC is exactly satisfied but this is a misleading statement (Sobey 1988). Dean has adopted a multi-step solution algorithm that decouples the KFSBC from the balance of the problem formulation and assumes that  $k$ ,  $R$ ,  $Q$  and the  $B_j$  coefficients are given parameters, equated to the most recent estimates from earlier steps in the iterative algorithm. This is a significantly weaker statement that cannot be categorized as exact. KFSBC errors as defined by Equation 19 will remain.

Single number measures of these boundary condition error traces are conveniently provided by the root-mean-square values (Dean 1974), as

$$\epsilon_{KFSBC} = \frac{1}{J+1} \sum_{j=0}^J K^2(x_j) \tag{21}$$

and

$$\epsilon_{DFSBC} = \frac{1}{J+1} \sum_{j=0}^J D^2(x_j) \tag{22}$$

where the  $x_j$  are evenly spaced between crest and trough and  $J$  should significantly exceed  $M$ ;  $J=100$  was adopted throughout. Note however that these error measures will be artificially small if  $J$  is chosen to correspond with the surface nodes, e.g.  $J = M = N$ .

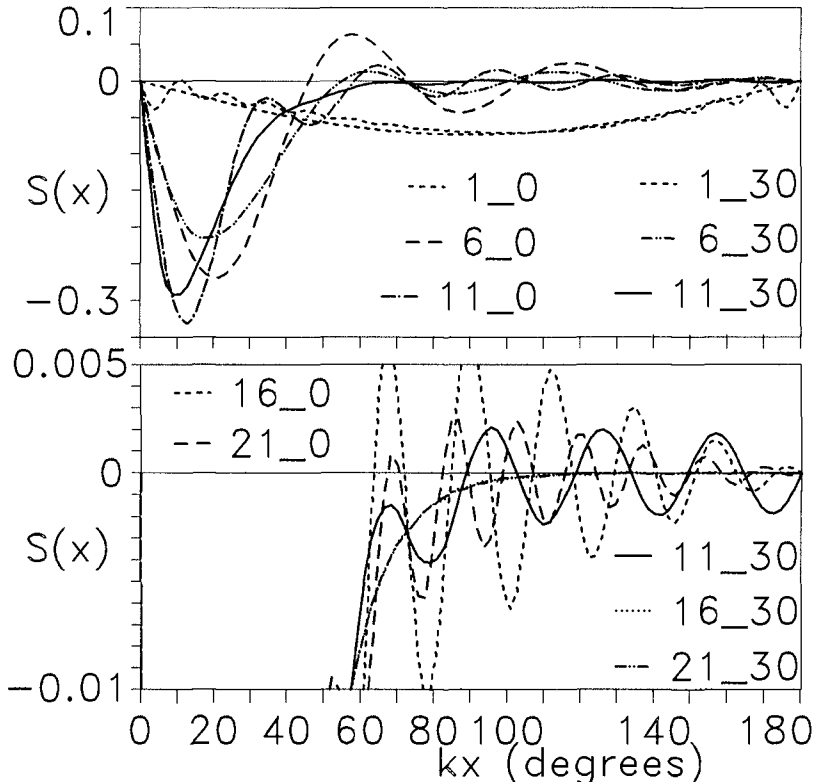


Figure 3 Slope Traces for Case 3C

The influence of the truncation order is implicit in the free surface boundary condition errors which provide a measure of a satisfactory numerical solution but not an especially direct measure of just what is a satisfactory physical solution. The direct influence of truncation order is rather more apparent from specific consideration of the truncated Fourier series approximation. Fourier series approximations to near sinusoidal profiles are quite trivial but the sharpening of the crest profile and flattening of the trough profile, that is experienced for higher waves in deep water and almost all waves in shallower water, requires a rapidly increasing truncation order. Insufficient Fourier terms will result in the Gibbs phenomenon and non-physical profile oscillations. In principle, a physical wave profile should be monotonically decreasing from crest to trough; the profile slope  $S(x) = d\eta/dx$  should never be positive. Figure 3 shows water surface slope traces for the same Dean case 3C solutions as in Figures 1 and 2, except that the Dean tabulated solution does not provide this information. The slope traces assist in identifying profile oscillations in the long flat trough profiles. Where the truncation order is insufficient, the slope traces oscillate above and below the zero level. These slope traces are especially sensitive to truncation order and overspecification and an additional error measure is provided by the positive area under the slope traces

$$\epsilon_{Slope} = \int_0^{L/2} \left[ \frac{d\eta}{dx} \right]_{+} dx \quad (23)$$

the + subscript indicating the inclusion of only those segments of the profile where  $d\eta/dx \geq 0$ . Physically satisfactory solutions should have a zero slope error.

Collectively, the KFSBC, DFSBC and water surface slope errors provide a reasonably comprehensive measure of the analytical veracity of a Fourier wave solution. In addition, the slope errors provide an excellent indication of the physical suitability of a computed solution.

## NUMERICAL EXPERIMENTS

Any Fourier wave solution is in principle dependent on three physical parameters wave height  $\omega^2 H/g$ , water depth  $\omega^2 h/g$ , and current  $\omega C_v/g$  or  $\omega C_s/g$  and on two numerical parameters truncation order  $N$  and overspecification  $MN$ . The three integral error measures defined above are then dependent on these five parameters. The details would be available from a comprehensive range of numerical. Each of these solutions is computationally intensive and exhaustively covering this five parameter space would be a massive computational task. A representative yet still reasonably comprehensive set of solutions were undertaken, based essentially on Dean case C at 75% of an empirical depth-dependent breaking wave height and  $\omega C_v/g = 0$ . Water depth  $\omega^2 h/g$  values included Dean cases 3 ( $\omega^2 h/g = 2\pi/100$ ), 4 ( $2\pi/50$ ), 5 ( $2\pi/20$ ), 6 ( $2\pi/10$ ), 7 ( $2\pi/5$ ), 8 ( $\pi$ ) and 10 ( $4\pi$ ). Case A solutions at 25% of an empirical depth-dependent breaking wave height were also computed for depth cases 3, 6 and 10. For each of these ten wave height - water depth combinations, solutions were computed for truncation orders  $N = 1(5)21$  and overspecification  $MN = 0(10)30$ ;  $MN$  extended from 0(10)50 for cases 3C, 4C and 7C. A total of 230 separate Fourier wave solutions were completed, which collectively provide an overall perspective on the  $N$  and  $MN$  dependence throughout the practical range of wave height and water depth values.

For each Dean case there are 20 or 30 separate solutions and results are conveniently presented as three dimensional bar charts for each dimensionless integral error measure and each Dean case. Even so there are 30 such plots and only selected examples can be included. The previous discussion has highlighted Dean case 3C and Figures 4, 5 and 6 show the corresponding integral error plots for the DFSBC, the KFSBC and the slope. As an aide to interpretation, these dimensionless plots are all to the same scale. They are truncated at  $10^{-6}$ , a convenient number that does not absolutely identify a successful solution but is strongly suggestive of one.

Figure 4 for the DFSBC shows a dependence on both truncation order and overspecification as anticipated by Figure 1. For  $MN = 0$ , there is a steady decrease in the rms error with increasing truncation order. Increasing overspecification has an immediate influence in significantly decreasing the rms error; further increases in  $MN$  have limited influence. The nature of this presentation however is rather deceptive of the computational effort involved. Computational effort is directly related to  $(2M + 6)^2$ , where  $M = N + MN$ . Designating computational effort as  $E^2$ , truncation order and overspecification are related as

$$N + MN = E - 6 \quad (24)$$

which can be represented on Figure 4 as straight line lines intersecting both the  $N$  and  $MN$  axes at the same numerical values. The dashed lines on the base plane of Figure 4 indicate lines of equal computational effort, which put the combined influence of both  $N$  and  $MN$  in better perspective. As perhaps expected, the rms error is rather more directly related to computational effort (i.e.  $N + MN$ ) than to either  $N$  or  $MN$  separately. Increasing  $MN$  alone may lead to a spurious result as the rms error very rapidly reaches a plateau level. Increasing  $N$  alone however leads to a consistent decrease in the rms error. It is apparent that truncation order is the crucial parameter. Overspecification can provide some measurable advantages but arguably no more (and potentially much less) than an equivalent increase in the truncation order to achieve the same computational effort.

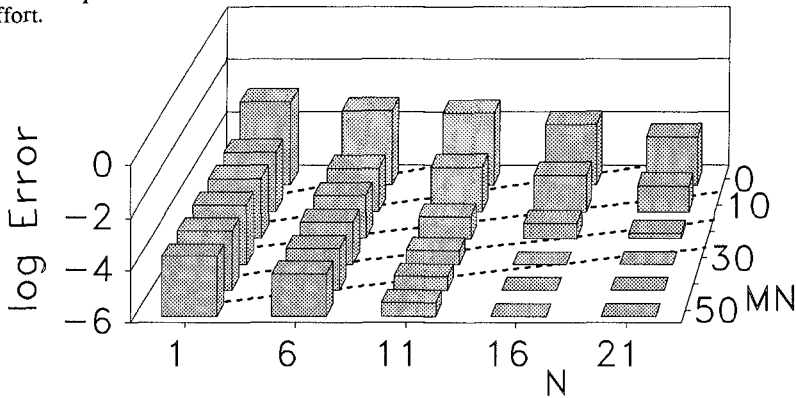


Figure 4 Rms DFSBC Error for Case 3C

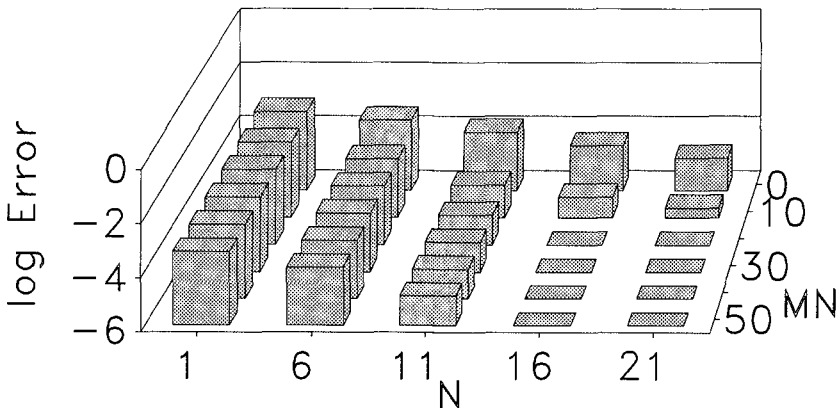
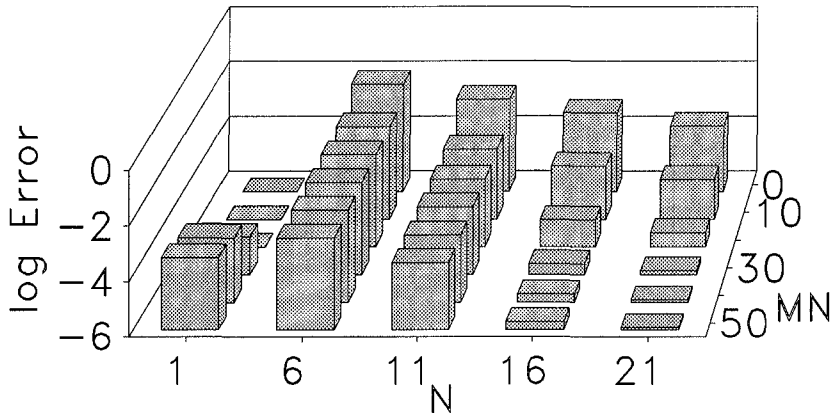


Figure 5 Rms KFSBC Error for Case 3C



**Figure 6 Slope Error for Case 3C**

Figure 5 for the KFSBC shows a very similar trend as does Figure 6 for the water surface slope. The base levels at  $N = 1$  are clearly spurious solutions; they predict a near-sinusoidal wave as is apparent from the equivalent slope traces in Figure 3. The overall picture presented by each of the three integral error plot is very similar, but there is one essential difference however. The rms errors in the free surface boundary conditions must approach zero asymptotically, whereas the slope error may suddenly jump to zero at finite values of the rms boundary errors. At the  $10^{-6}$  level, oscillations in the trough profile at barely perceptibly and certainly define a pragmatic solution. Higher cutoff levels may in fact be acceptable. It would appear nonetheless that the slope summary plot provides a useful measure of an acceptable solution, both mathematically and physically.

Space limitations preclude presentation of all the summary plots. Sufficient detail is provided by one of the rms error plot (say DFSBC) together with the slope plot. Figure 7 shows these error plots for Dean case 3A ( $\omega^2 h/g = 2\pi/100$ ;  $\omega^2 H/g = 0.01224$ ,  $C_p = 0$ ) at 25% of the empirical breaking wave height. The significantly lower wave height is much less demanding of the Fourier wave theory and the  $10^{-6}$  base levels are rapidly achieved for both the rms DFSBC error and the slope error.

Figure 8 through 14 shows the summary plots for Dean cases 4C, 5C, 6A, 6C, 7C, 8C and 10C respectively. These plots clearly demonstrate the relative ease with which acceptable solutions are achieved in deeper water. Case 4C (Figure 8) follows a very similar trend to Case 3C but profile steepness is not quite as extreme in the slightly deeper water and the  $10^{-6}$  base level is reached with somewhat less computational effort. Case 5C (Figure 9), 6C (Figure 11) and 7C (Figure 12) continue this trend, slope errors becoming rapidly less problematic. In fact, slope errors appear not to be a serious problem in deeper water. A comparison of Case 6A (Figure 10) and Case 6C (Figure 11) once again demonstrates the relative ease with which Fourier solutions are achieved at lower wave heights.

The Case 8C (Figure 13) summary plot continues these trends in very deep water, except that the DFSBC (and also the KFSBC which is not included) errors reveal an additional problem at  $N = 21$ ,  $MN = 0$ . The Case 10C solution (Figure 14) follows the same trend but not the Case 10A solution (not included). Perusal of the solution details reveals that this apparent problem is a consequence of finite compiler and machine precision. The Fourier coefficients become very small very rapidly in deep water and the higher coefficients are typically fifteen orders of magnitude smaller than the leading  $B_1$  coefficient. This confronts the capabilities of double precision arithmetic (REAL\*8 variables in Fortran), although this is both compiler and machine dependent. In such a

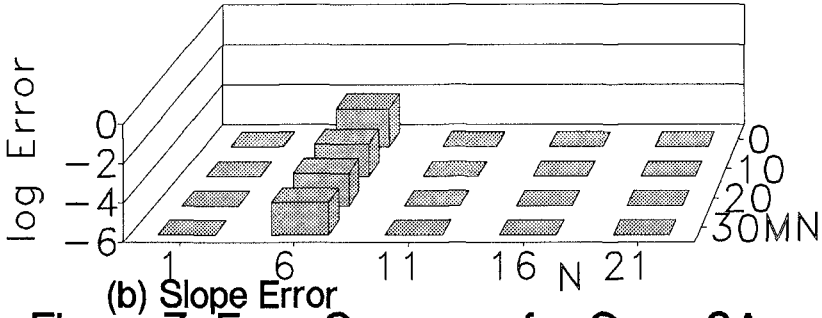
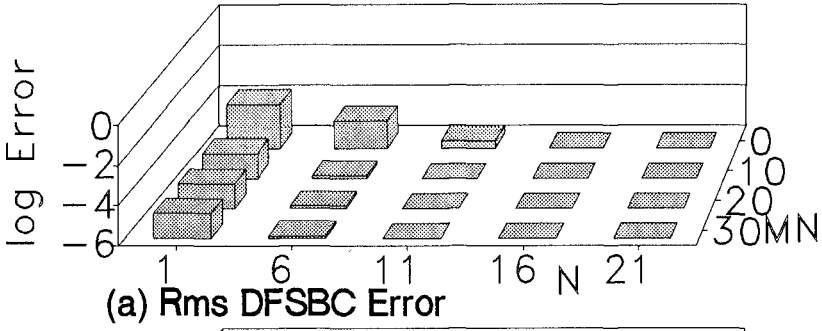


Figure 7 Error Summary for Case 3A

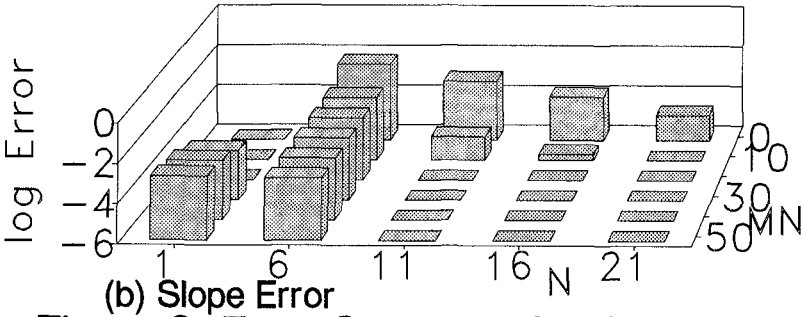
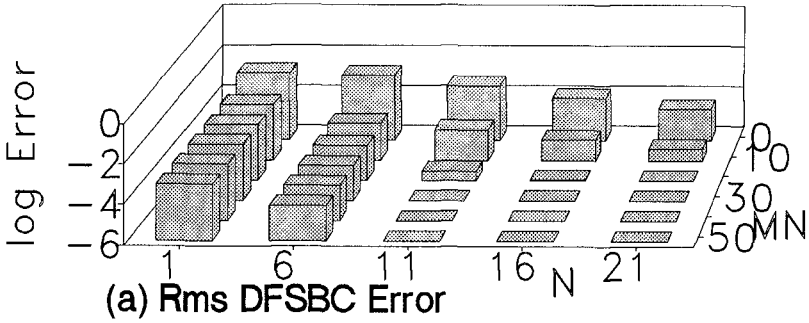


Figure 8 Error Summary for Case 4C

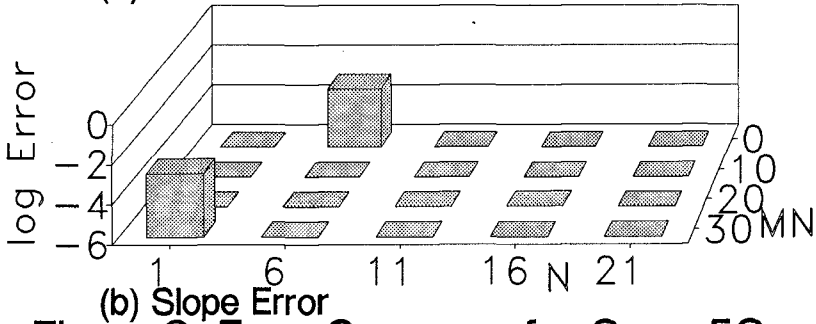
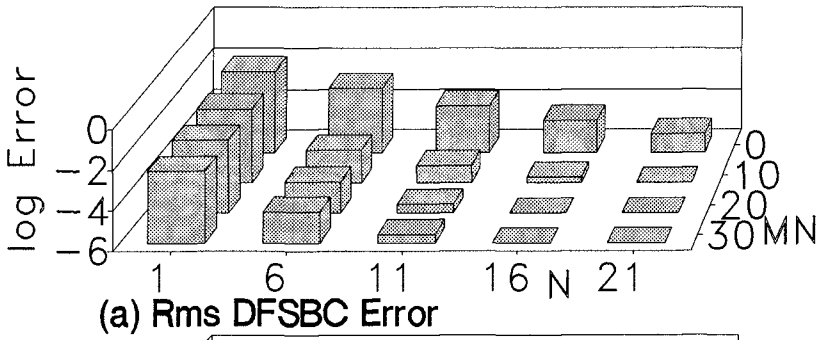


Figure 9 Error Summary for Case 5C

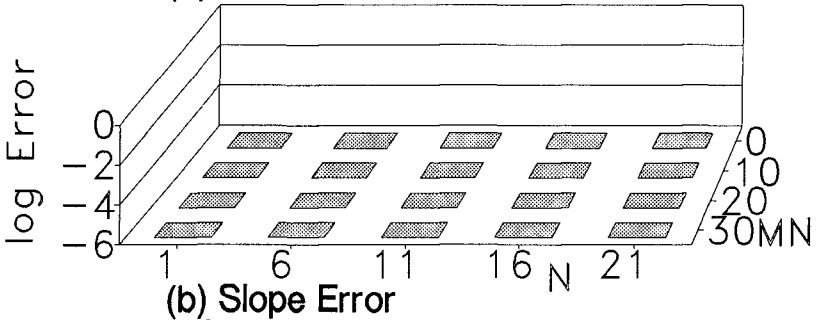
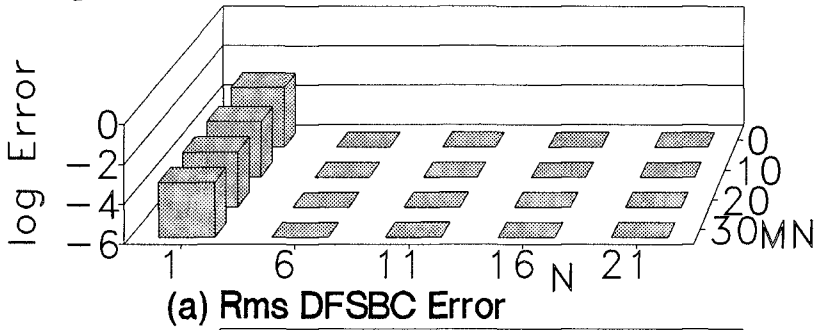


Figure 10 Error Summary for Case 6A

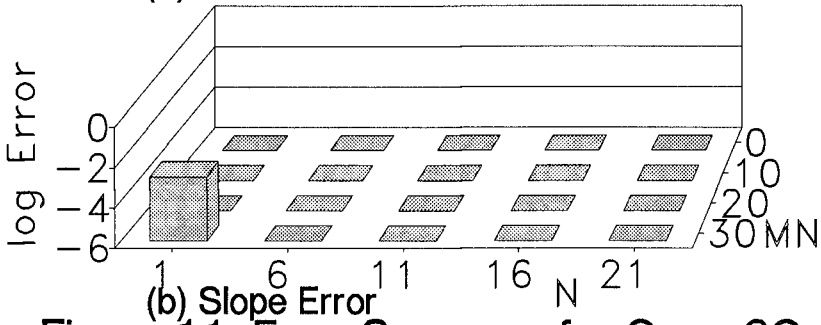
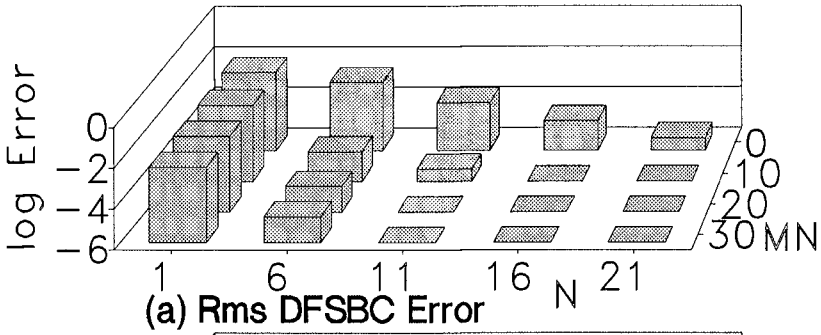


Figure 11 Error Summary for Case 6C

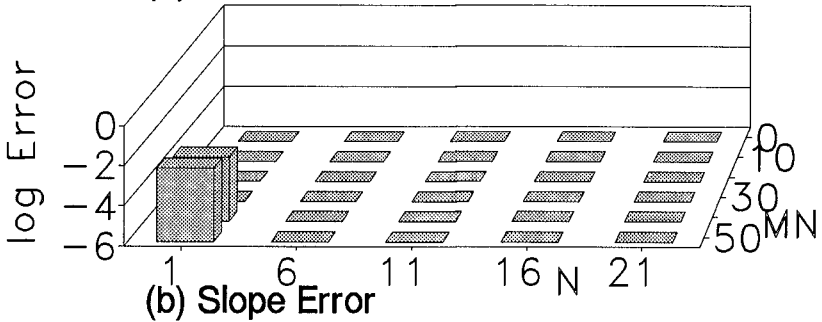
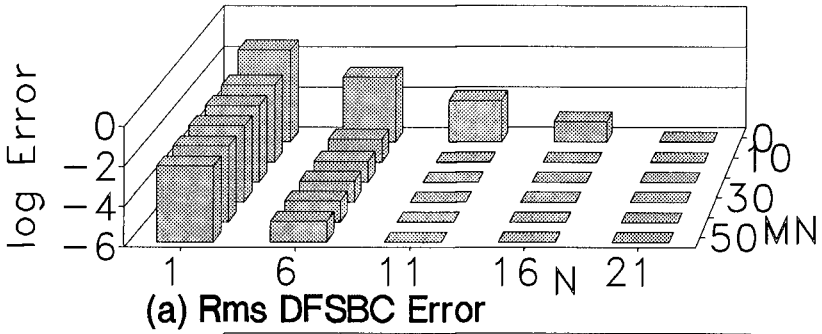


Figure 12 Error Summary for Case 7C

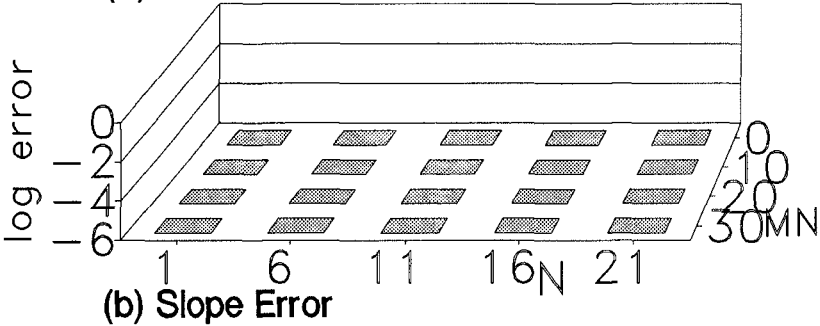
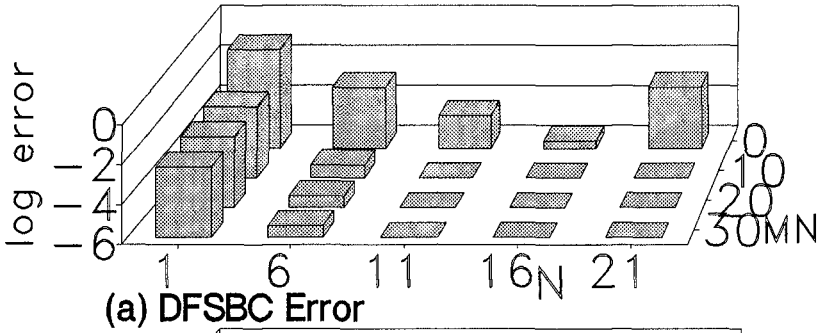


Figure 13 Error Summary for Case 8C

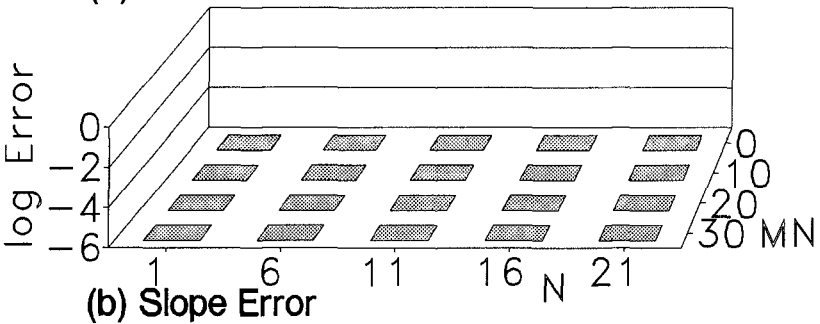
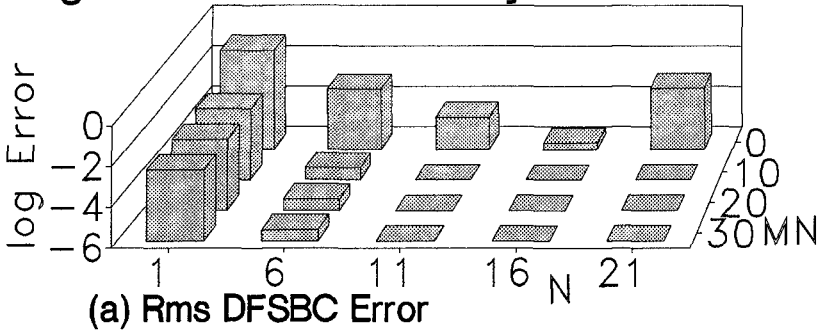


Figure 14 Error Summary for Case 10C

case it is possible to adopt too high a truncation order, very much the reverse of the more serious problems in shallower water. A truncation order of 21 is unnecessary in deep water.

In the application of analytical wave theories such as Stokes and cnoidal, the choice of an appropriate order is a matter of engineering judgement, and depends upon the nature of the physical problem, the required precision of the computation and sometimes on overriding regulatory requirements. The choice of truncation order and overspecification for Fourier wave theory is similarly a matter of engineering judgement and it is not appropriate to nominate specific values. The consequences of a particular choice however can be evaluated from the range of summary plots presented that have been presented.

## CONCLUSIONS

Each Fourier wave solution is nominally dependent of three physical parameters, wave height  $\omega^2 H/g$ , water depth  $\omega^2 h/g$ , and current  $\omega C_v/g$  or  $\omega C_s/g$  and on two numerical parameters truncation order  $N$  and overspecification  $MN$ . Specific attention has been given to the solution dependence on  $N$  and  $MN$  and to the distinction between a successful numerical solution and a successful physical solution.

Some 230 separate Fourier wave solutions have been completed over a wide parameter range representative of field conditions. Trends are summarized in terms of three integral error measures, the rms DFSBC and rms KFSBC errors, which are measures of a successful numerical solution, and a slope error, which is a measure of a successful physical solution. A dimensionless cutoff level of  $10^{-6}$  has been adopted to identify a successful solution. Precision is shown to be closely related to computational effort ( $N + MN$ ) but the truncation order  $N$  is the dominant parameter. There is some minor advantage in a little over specification but significant overspecification does not enhance precision.

A range of summary error plots should assist in the rational assignment of truncation order and possible overspecification for Fourier wave solutions.

## REFERENCES

- Chaplin, J.R. (1980) "Developments of stream-function wave theory". Coastal Engineering, 3, 179-205.
- Dalrymple, R.A. (1974) "A finite amplitude wave on a linear shear current". Journal of Geophysical Research, 79, 4498-4504.
- Dean, R.G. (1965) "Stream function representation of nonlinear ocean waves". Journal of Geophysical Research, 70, 4561-4572.
- Dean, R.G. (1974) "Evaluation and development of water wave theories for engineering application". U.S. Army Coastal Engineering Research Center, Report SR-1, 2 volumes.
- Fenton, J.D. (1983) "The numerical solution of steady water wave problems". Manuscript.
- Rienecker, M.M. and Fenton, J.D. (1981) "A Fourier approximation method for steady water waves". Journal of Fluid Mechanics, 104, 119-137.
- Sobey, R.J. (1988) "Variations on Fourier wave theory". Manuscript under review.